Analytic Element-Finite Volume Based Coupled Groundwater-Surface Water Interaction model for Canal Command Systems

Komal Kumari[1] · Anirban Dhar[2]

Abstract

Regional scale modeling of coupled groundwater-surface water interaction in canal command areas is difficult due to high computational requirements and data insufficiency. Groundwater plays an essential role in the interaction process to fulfil the irrigation requirement in tail reaches of canal command areas. A comprehensive coupled model is required to simulate the canal command systems by incorporating the processes: (a) saturated groundwater flow, (b) unsaturated flow and (c) overland flow. In the present work, a fully-coupled model is developed that simulates saturated groundwater flow using Analytic Element Method (AEM), unsaturated flow using analytical solution and overland flow using Finite Volume Method (FVM) based Zero-inertia model. The Capability of the developed coupled model is demonstrated for Damodar Left Bank Main Canal (LBMC) under two canal regulation scenarios for "Boro Rice" cultivation season (Jan-Apr). Major canal water shortage is observed in LBMC during this season. It can be observed from the results that hydraulic heads in the upper reach are quite high whereas it is significantly lowering down as we move away from the main canal or in the lower reach where the groundwater is the main source of Boro rice irrigation. The considerable decline in hydraulic head values can be observed in LBMC which can be justified with a decrease in water supply and an increase in the area under Boro rice cultivation.

1 Introduction

Water management in canal command areas is an important issue. Canal water shortage is observed in the tail reaches of rice-dominated canal command areas due to uneven distribution of water. Consequently, over-exploitation of groundwater is occurring which may

✉ Komal Kumari
ugetkomal@gmail.com

Anirban Dhar
anirban@civil.iitkgp.ac.in

1   Department of Civil Engineering, Birsa Institute of Technology Sindri, Dhanbad, India

2   Department of Civil Engineering, Indian Institute of Technology Kharagpur, Kharagpur, India

affect the sustainable use of water resources. Therefore, a comprehensive coupled model is required for sustainable water resources management in the canal command system by incorporating the processes: (a) saturated groundwater flow, (b) unsaturated flow and (c) overland flow.

Modeling in canal command systems are regional scale problems. Groundwater flow in regional scale aquifers (Bakker et al. 1999; Craig et al. 2006) can be modeled using AEM. The challenge of modeling regional scale problems with limited data sets can be addressed with the Analytic Element Method (AEM) based model. AEM, developed by Strack during 1980s (Strack 1989), provides the analytic solutions to groundwater flow problems, using superposition of solutions (elements) of governing differential equations of flow. It was not designed to replace gridded models, however, there are several situations (e.g., regional groundwater flow problems) where AEM was found to be more convenient than other numerical methods (Omar et al. 2019; Kumari and Dhar 2020; Tong et al. 2023). In contrast to grid-based methods, AEM does not require construction of grids and provides a solution for hydraulic head at every point within the model domain, instead of only at the grid nodes. The computational effort in AEM models is directly proportional to the number of features considered in the model domain and their discretization level. It does not get much influenced by the areal extent of the domain making it more convenient to model the main features of large geological areas at high resolution in low computational time (Bandilla et al. 2007).

Overland flow generated by basin irrigation can be accurately solved using the complete hydrodynamic equations which is based on the principle of mass and momentum conservation equations (Walker and Merkley 1994; Murillo and García-Navarro 2010; Zhao and Liang 2022). The hydrodynamic models are highly accurate but expensive to solve due to its mathematical/computational complexity (Murillo and García-Navarro 2010; Zhang et al. 2014). Over the last few decades, many computationally efficient surface water models have been developed based on the simplified form of these equations to deal with the issue of high computational requirement. Zero-inertia model is the most widely used modeling technique for overland flow (Walker and Merkley 1994; Brufau et al. 2002; Philipp et al. 2012; Valipour 2012) which is based on the simplified form of complete hydrodynamic equations. A broad range of research studies focussed on the comparative analysis of zero-inertia and hydrodynamic models are available in the literature (e.g., Cea et al. 2010; Zhang et al. 2014; Aricò and Nasello 2018). The applicability of the zero-inertia model (Schmitz and Seus 1992; Philipp et al. 2012; Zhang et al. 2014; Zhang et al. 2017; Caviedes-Voullième et al. 2020) can be well justified for the cases in which water depth is significantly lesser than the horizontal extension of flow. The main advantage of 2D zero-inertia model over other shallow water equations is its conceptual and mathematical simplicity which needs lesser computation time per time step.

Surface water and groundwater interaction process are quite influenced by the way of incorporating surface water features in the groundwater model. AEM is preferably used to simulate groundwater flow at regional scale in the interaction process owing to its flexibility while applying boundary conditions (De Lange 1999; Omar et al. 2019). Surface water act as a boundary in the groundwater flow model. These surface water features can be modeled considering it in full contact with the aquifer, or separated from it by a leaky layer (Fitts 1989; Strack 2003; De Lange 2006; Strack 2006; Bakker 2007). There are several important research that analyzed the conjunctive use of water in command areas (Murray-Rust and Vander Velde 1994; Biswas et al. 2017; Omar et al. 2019; Jha et al. 2020; Ahmad and Zhang 2022; Pradhan et al. 2022) by different techniques but only a few of them are fully-coupled.

It is evident that individual models for describing each component of the command area systems, e.g., steady/unsteady overland flow, infiltration in the unsaturated zone, and groundwater movement in the recharged unconfined aquifers are available. However, there are very few fully-coupled models linking all the components together. Further, the coupled model incorporating AEM based groundwater flow model and FVM based surface water flow model is not present in literature. Command area system model requires return flow calculation in its framework. An integrated canal command system simulation model is proposed that can simulate saturated groundwater flow using AEM, unsaturated flow using analytical solution and overland flow using FVM based Zero-inertia model. The proposed model considers Green-Ampt equation to model the interaction between surface water and groundwater model.

2 Mathematical Conceptualization of Surface Water Flow Model

This research work attempts to consider the surface water flow movement from one cell to another, infiltration, evapotranspiration, rainfall taking place in the basins, and the recharge (both direct and indirect) and the discharge of the underlying groundwater body. For the ease of numerical computation, one assumption has been made here that it does not consider bund or dyke between two consecutive cells which exist in reality. However, to compensate with this limitation, a relatively high value of Manning's roughness co-efficient was considered (Zapata and Playan 2000; Valipour 2012). It can also be justified with the presence of irregularities in the soil surface elevation in the real field. The movement of water from the watercourses to the fields is assumed to fill a cell up to the specified water level (equal to the standing water requirement of Boro rice) and then overflow to the next cell. Two-dimensional zero-inertia equation is used as the governing equation.

$$\frac{\partial h}{\partial t} - \nabla \cdot \left[\lambda_w(h)\nabla(h+z)\right] = R_n \tag{1}$$

h = Water depth, $\lambda_w(h)$ = Diffusive co-efficient of surface water, z = bed slopes of the bottom level and R_n = Rainfall intensity. Cell centered Finite Volume discretization is used here to discretize above Eq. (1) (please refer supplementary file for detailed description of discretization). Each cell in the model domain is considered as a control volume C_v.

$$\int_{C_v} \frac{\partial h}{\partial t} dC_v = \int_{C_v} \nabla\left[\lambda_w(h)\nabla(h+z)\right] dC_v + \int_{C_v} R_n dC_v \tag{2}$$

2.1 Mesh Generation

The unstructured triangular (UT) cells were used for domain discretization. Mesh generation at a regional scale using a standard mesh generation framework is a challenging problem. The local refinement of mesh near the hydrogeologic features of interest plays an important role while dealing with regional scale problems having large number of hydrologic features as well as large number of cells. To address this problem Gmsh (Geuzaine and Remacle 2009) was utilised to generate 1D (to represent canals) and 2D (to represent surface flooding) meshes simultaneously by embedding point/line in surface. The area, centroid and neighbouring cells of each cell were calculated/identified using the python code, after reading the mesh file in it.

2.2 Initial and Boundary Conditions

Initially all the spatial cells in the model domain were considered to be dry. However, zero water depth in the above equation may result in a singular solution. Therefore, a minimum positive value (10^{-6}) was initially assigned to the depth of flow in the model domain. To start the numerical simulation, the initial value of water depth (bed elevation $+10^{-6}$) was specified at each cell. The land surface elevation was also specified as the initial condition. Hence, the hydraulic gradient was also assigned a minimum value for the cases when it becomes zero. λ_w (diffusive coefficient) is a function of the reciprocal of the hydraulic gradient. Thus, a minimum value (10^{-6}) was assigned for zero slope conditions to avoid the singularity problem.

The external boundary conditions for the cells along the four sides of the model domain were no-flow (Supplementary Fig. S1-(a)). No cells along the boundary were receiving water from other sources except their adjacent cells and rainfall if considered. Line inflow (flow through canals) was imposed as the internal flow boundary condition (Supplementary Fig. S1-(b)) to model the inflow from the canal to the cells in the model domain. The water surface elevation in the canal was acting as a boundary condition to the inflow side of the cell lying along the canal lines.

2.3 Numerical Stability

The investigation of stability conditions in the numerical simulation model is necessary for achieving feasible results. The Numerical stability of an explicit scheme mainly depends on the choice of optimal time step (small enough to achieve numerical stability and large enough to maintain the computational efficiency of the model). However, the choice of optimal time step depends on Manning's roughness coefficient, free surface gradient, water depth and mesh size of the model domain (Hunter et al. 2005). A proper mesh size selection also plays an important role in the numerical stability and computational efficiency of the solution. The optimal time step for explicit schemes was selected based on the following expression (Cea et al. 2010):

$$\triangle t < \triangle x^2 \frac{n}{h^{5/3}} \sqrt{\frac{\triangle z_s}{\triangle x}} \tag{3}$$

where $\triangle t$ = time step, $\triangle x$ = cell/mesh size, h= water depth, and $\triangle z_s$ = free surface gradient, and n=Manning's roughness coefficient. It can be observed from Eqn. 3 that with the increase in the value of Manning's roughness coefficient the stability of the solution increases. A value of 0.15 ($s/m^{1/3}$) was selected for the Manning roughness coefficient to minimize the effect of irregularities in the soil surface elevation and vegetation cover in the field/model domain (Zapata and Playan 2000; Valipour 2012).

2.4 Convergence Criteria

The convergence of the simulated result is analysed with the root mean square error (RMSE) using the expression given below:

$$RMSE = \sqrt{\frac{\sum_{P=1}^{N_p} \left(h_{sp} - h_{rp} \right)^2}{N_p}} \tag{4}$$

where h_{rp} and h_{sp} are reference and simulated flow depths, respectively. The reference flow depth was obtained in the last time step with the initial specified value. N_p is the total number of cells considered for the numerical simulation. The simulation model performs iteration until the value of error (RMSE) is lower than the tolerance value specified (10^{-6}). Moreover, if the obtained value is smaller than the initial flow depth ($10^{-6}m$), it is reset to the initial specified value to avoid the singular solution of the numerical model introduced by negative or zero flow depth.

3 Unsaturated Zone Modeling using Green-Ampt Model

Overland flow is generated due to basin irrigation or rainfall, advances in both x- and y-directions on an initially dry bed of the basin. Throughout these processes of water wave-front movement and subsequent ponding, most of the water is lost by infiltration. A part of the infiltrated water is utilised by crops/plants that are cultivated in the basin and another part contributes to recharge the underlying unconfined aquifer.

It may be recalled that although overland flood irrigation is suitable for other types of crops as well, present work considers Boro rice cultivation only which requires standing water in the fields. The unsaturated zone acts as the medium to exchange water in terms of recharge, evapotranspiration and infiltration between surface water and groundwater. It controls the interaction process through one-dimensional vertical movement of water. There exists a range of infiltration models to simulate one-dimensional vertical movement of water: empirical/semi-empirical models (e.g., Kostiakov's Equation, Horton's Equation, Philip's Equation) and physically based models (e.g., Richard's equation, Green-Ampt method). Among the physically based models, the Green-Ampt method (proposed by Green and Ampt in 1911) is found out to be the most suitable for the estimation of infiltration through homogeneous/heterogeneous soil under surface ponding conditions (please refer to supplementary file for the detailed mathematical conceptualization of Green-Ampt approach used here).

4 Validation

The performance of the surface water-unsaturated flow model is evaluated using the Southeast corner flow problem (SEC) of Walker and Merkley (1994), in which spatially varied infiltration and Kostiakov-Lewis equation were considered for infiltration rate computations. However, we are using uniform infiltration (averaged value of spatially varied infiltration parameters) and GA infiltration model. Appropriate values of GA parameters are selected using Rawls et al. (1983) for the same infiltration rate achievement with the given parameters of Kostiakov-Lewis equation. A hypothetical basin irrigation system (100 m×100 m) with inflow discharge of 0.1 m^3/s for 100 min of application time and Manning's roughness co-efficient value of 0.04. For the present test case model domain is discretized with total of 1024 cells of $5m \times 5m$ cell size. The contour map of simulated overland flow after 30 *minutes* and 60 *minutes* is shown in Supplementary Fig. S2.

5 Regional Scale Surface Water-Groundwater Interaction Model

Regional scale surface water-groundwater interaction model still remains challenging due to the complex nature of groundwater systems, and computational limitations associated with real field application. As discussed in the literature review section, almost all the overland flow models were focused on the movement of the water front in the command area and consider only the loss of water due to infiltration. They did not consider the contribution of pumped groundwater in the water-deprived canal command areas in a fully-coupled framework. In the present work, an overland flow model for flood irrigation in Boro rice is proposed, which requires sufficiently high standing water for its maturity and proper yield. Further, the cultivation of high water demanding Boro rice in the water-scarce zones (mid and lower reaches) of the command area during the Boro season (rainfall approximately less than 10% of average annual rainfall) intensify the water shortage problems in these zones. Subsequently, it gives rise to excessive groundwater pumping which ultimately causes significant drops in groundwater levels in the command area.

5.1 Study Area

The gross command area of the Damodar valley irrigation system comprises 568778 hectares with a culturable command area of 393964 hectares. The major portion of the command area (80%) lies in the left bank of Damodar river. LBMC of Damodar river is considered here as the study area which is spread over total of 28 blocks: 17 blocks of Bardhaman district, 8 blocks of Hoogly district, and 3 blocks of Howrah district in the state of West Bengal. The study area is confined between $22°33'0''$ N to $23°41'0''$ N lalitudes and $87°22'$ E to $88°30'0''$ E longitudes. The location map of the study area is shown in Fig. 1. Detailed information about the study area can be found in Pradhan et al. (2022b)

LBMC was initially designed to fulfill water requirements for Rabi (October - March) and Kharif (July - October) crops only. However, after the introduction of Boro rice (high water consuming crop) cultivation in the command area (Boro rice maps for year 2012 and 2013 are provided in Supplementary Fig. S3), water demand was considerably increased. Moreover, the overall efficiency of the canal networks was decreased due to reduction in canal carrying capacity and unauthorized human interference in terms of forceful control of gates in upper reaches. As a result, the farmers at the middle and tail ends are deprived of canal water, leading to water scarcity in these areas. Canal regulation maps (water supply maps) of 2012 and 2013 during the Boro season are delineated in the GIS platform using the water supply charts (collected from Damodar's head works division). Canal regulation maps of 2012 and 2013 are shown in Fig. 2a, b respectively. It can be observed from Figs. 2a, b that the water supply is limited to the canals in the upper reach and very few in the middle reach of the command area. Therefore, Boro rice cultivation in the major part of the command area is dependent on groundwater.

5.2 Coupled Modeling Framework

The coupled model was developed by connecting surface water, infiltration and groundwater models. The flow diagram for the working steps of the coupled model is shown in Fig. 3. The model starts from the algorithm indicated on the middle topmost part of Fig. 3 by initializing all parameters in 2D zero-inertia model. The overland flow depth generated
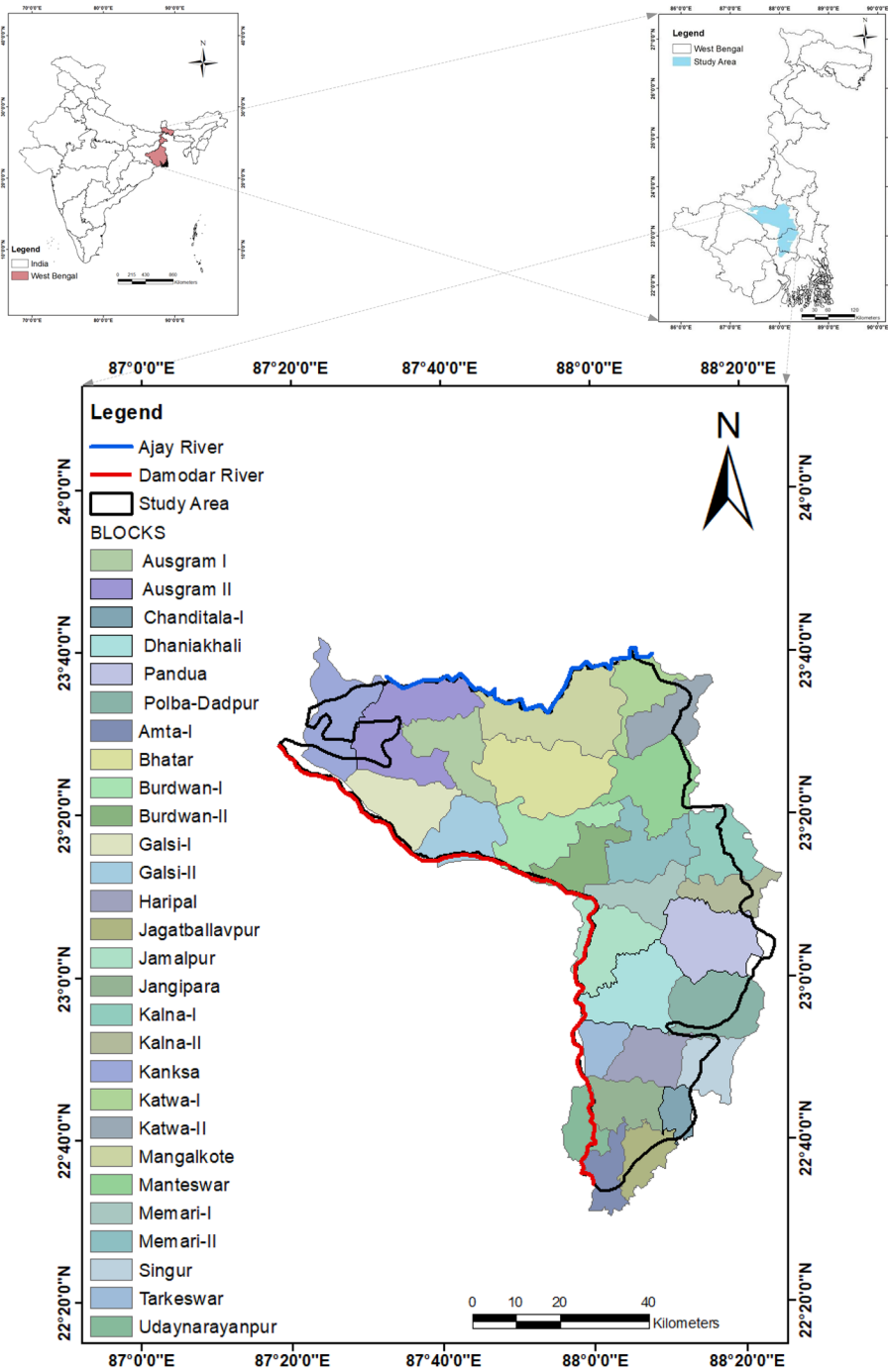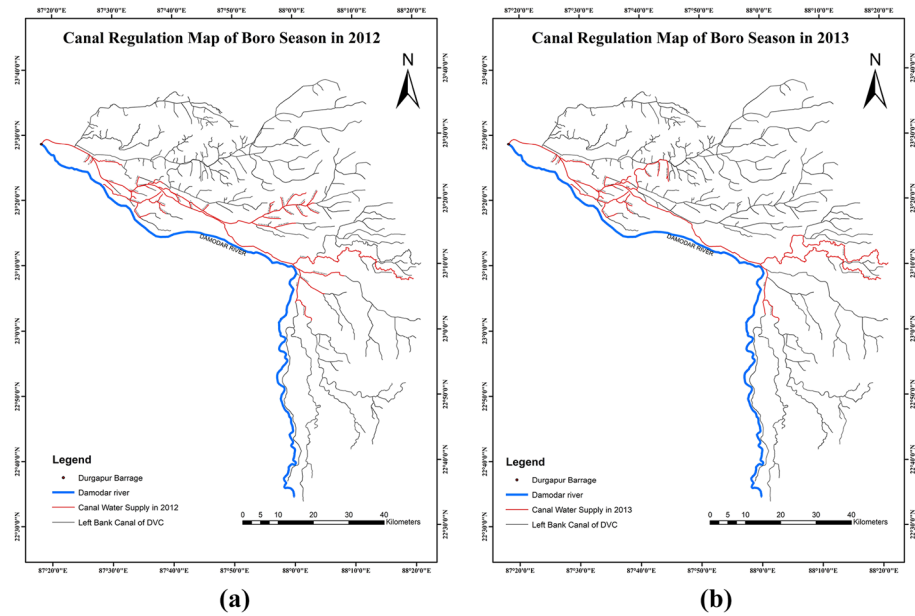
Fig. 1 Location map of study area

Fig. 2 Canal regulation map of LBMC command area for: **a** 2012, **b** 2013

due to basin irrigation with canal inflow, rainfall and evapotranspiration as input values, proceeds for inter-cell flow movement after identifying neighbouring cells and their type. In the processes of water movement and subsequent ponding, most of the water is lost by infiltration for the wet cells (cells with water level greater than the standing water requirement of Boro rice) and goes to the groundwater model as input (recharge). The standing water requirement of Boro rice is considered to be greater than or equal to 100 mm. It means a cell with flow depth greater than or equal to 100 mm was considered to be wet or otherwise dry. Moreover, for the dry cells, water deficit values were calculated based on evapotranspiration requirements and available rainfall values and updated in the same time step. Water deficit values were considered as the sink term for the groundwater model. After updating surface water depth, it will check for the achievement of convergence criteria (RMSE value should be less than tolerance value) to find out the updated variable at that time step. Simultaneously, AEM based groundwater model with Damodar river as the left boundary, Ajay river as the right boundary and discharge-specified canal segments as analytic elements along with recharge as inflow and pumped water as outflow was also run. Discharge-specified canals were acting as the source of indirect recharge to the groundwater model. The direct recharge and pumping are modeled using area sink in AEM. The time steps for the surface water model, infiltration model and groundwater model are not the same. The flow diagram for the working steps of the coupled model is shown in Fig. 3.

The coupled model calls the infiltration model in every alternate 5-time steps, which means if the time step for the surface water model is t seconds then the time step for the infiltration model will be 5×t seconds to minimize computation burden. Moreover, the time step for the groundwater model is in days owing to the long-term regional variations in groundwater variables. The response of the groundwater model was checked at an interval
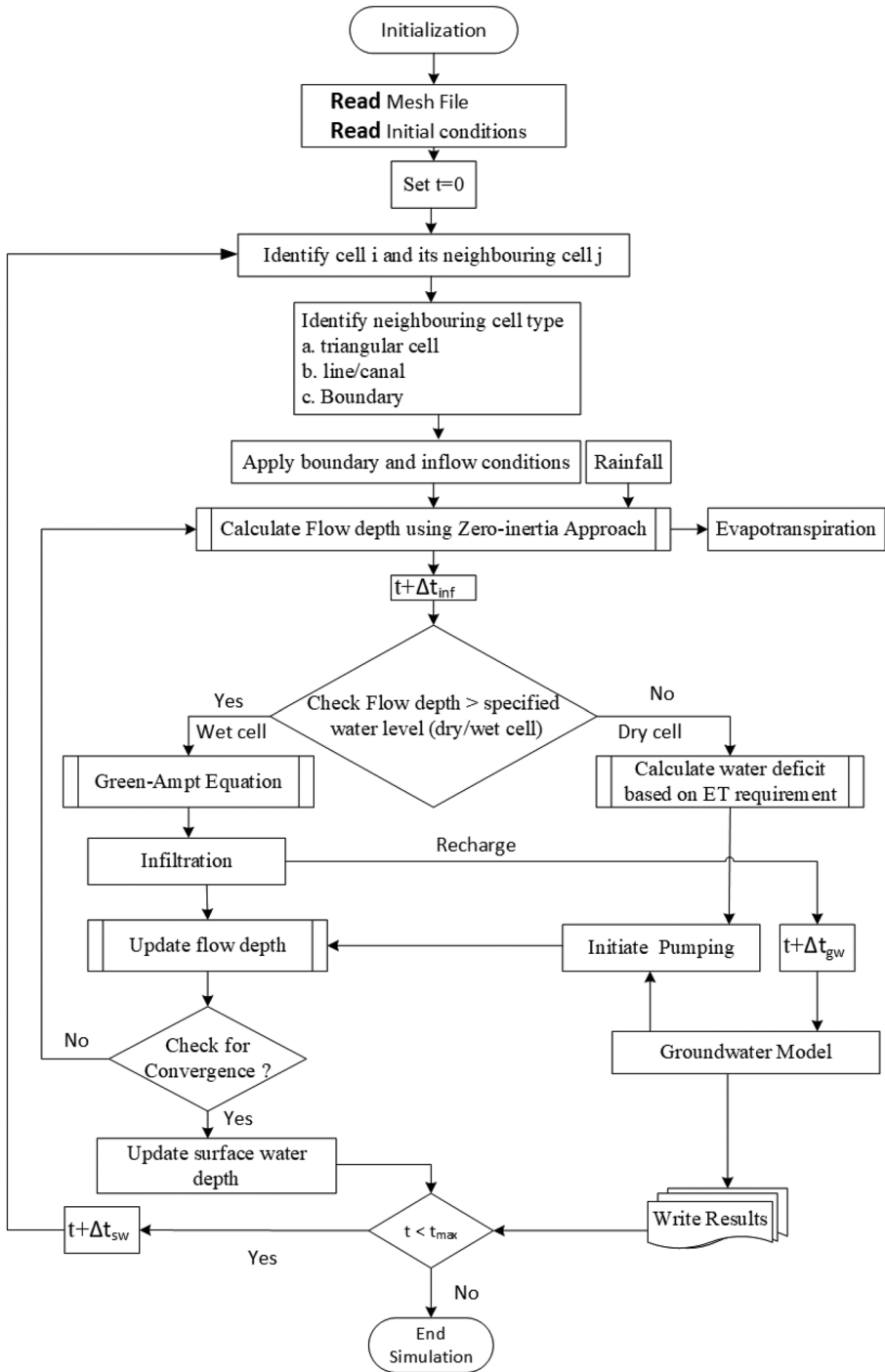
Fig. 3 Flow chart for the Surface Water-Groundwater interaction model

of 30 days only to observe significant changes in groundwater head. The aforesaid steps were repeated till the end of the simulation.

5.3 Input Parameters

The input parameters for the coupled model would include: (1) canal inflow to the basin cells as overland flow; (2) rainfall, if any, on the basin cells; (3) evapotranspiration rate of Boro rice; (4) the percentage of total area under Boro rice cultivation; (5) water supply charts during the Boro season for two regulation years (Fig. 2); (6) hydraulic boundary condition in terms of the head-specified line sink with Damodar river as the left boundary and Ajay river as the right boundary; (7) strength-specified line sink (discharge per unit length along main and branch canals by dividing it into small segments)and, (8) soil parameters as required for the unsaturated model.

Geomorphology wise this area is uniform in nature. Although local variations in soil parameters exist, an equivalent average value was considered for the groundwater simulation. There were considerably small variations in the values of soil/aquifer parameters. Therefore, the values of these parameters were assigned as the averaged value of 28 blocks. Soil is of clayey loam type with good water holding capacity (refer Supplementary Fig. S4 for soil map). The major part of the study area comprises fine soil and a small part with coarse loamy soil (Pradhan et al. 2022). The parameters of Green-Ampt model were approximated based on the soil type. Appropriate values of Green-Ampt parameters were chosen using Rawls et al. (1983).

Daily discharges to LBMC of Damodar River were collected and analyzed to calculate the average discharge during four months of simulation period. It was observed from the analysis of daily discharge data that maximum discharge was released during mid-February to the last week of March which is the development and mid-season stage of Boro rice. However, here we are considering constant discharge throughout the simulation period to avoid computational complexities. As we have the discharge data of main canal only, therefore the calculation of its distribution to different branch canals was worked out using the surveyed cross-section data (two surveyed cross-sections are shown in Supplementary Fig. S5 for reference).

Ajay river and Damodar river present in the study area were simulated as the specified-head line sink. Furthermore, the strength at each canal segment is specified in such a manner that the surface water level at the center of canal segments (also termed as control point) is equal to the piezometric head in the aquifer below it (Strack 1989). The strength-specified line sinks were serving as the Dirichlet boundary condition for the groundwater model. Individual canals were divided into several small segments to specify strengths. The consideration of small surface water segments for specifying strength is quite important to get reasonable interaction between surface water and groundwater. Larger the length of surface water segments, the higher and more unrealistic exchange between these two was observed. We are not considering the inflow of groundwater to surface water as an unsaturated zone exists between the canal and aquifer. It may be noted that strength (σ) is positive for extraction per unit length and negative for infiltration per unit length. The nominal value of rainfall (100mm) during Boro season was considered as inflow to surface water model and 6mm/day of evapotranspiration value was considered as outflow from the surface model. The water requirement for Boro rice was considered to be equal to the standing water requirement (minimum 100 mm) plus evapotranspiration requirement (6 mm/day) minus the available rainfall values (100 mm for the Boro season).

The coupled model was run for two regulation years 2012 and 2013 with above defined input parameters. The results of the surface water model and coupled model for these two years are discussed in the subsequent sections.

6 Results and Discussion

The framework of the present model integrates all the individual processes (overland flow, infiltration, groundwater flow) taking place in a canal command area where conjunctive use of water is practised. The surface water supplied from a canal network to the command area through overland flow (cell-to-cell transfer) as well as precipitation if any. The cells that do not receive surface water were assumed to pump water from the underlying unconfined groundwater aquifer to meet the evapotranspiration requirement of the crop grown.
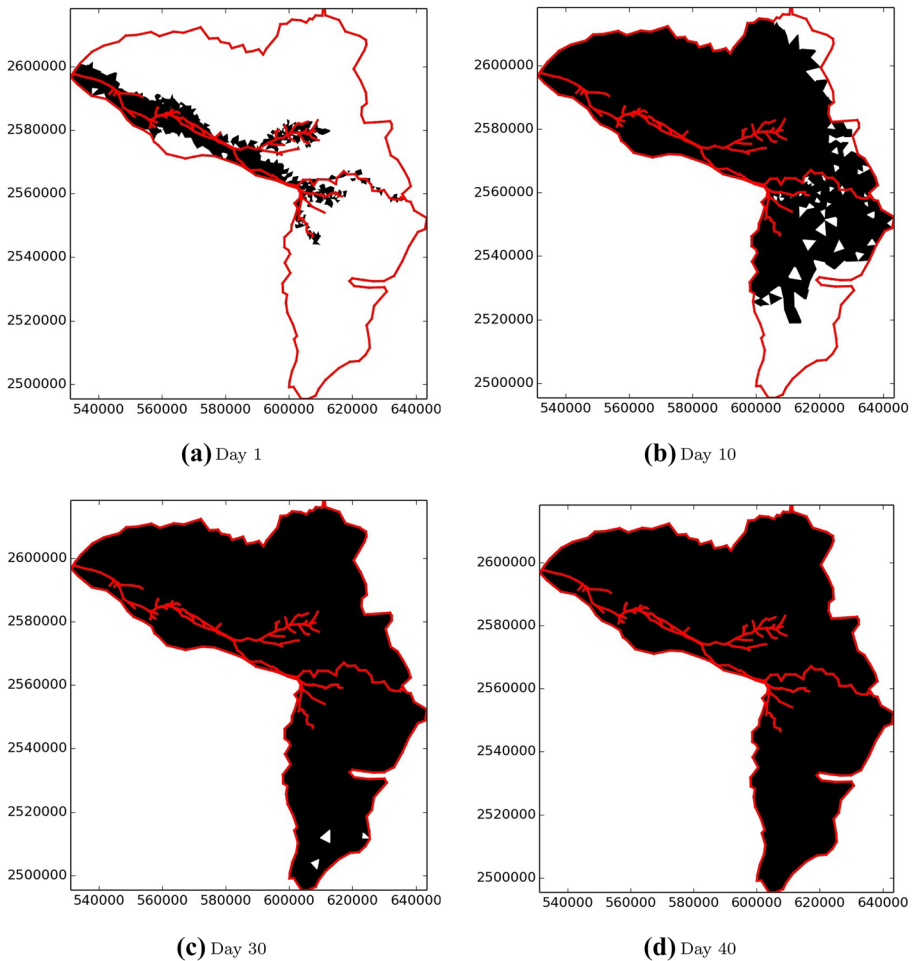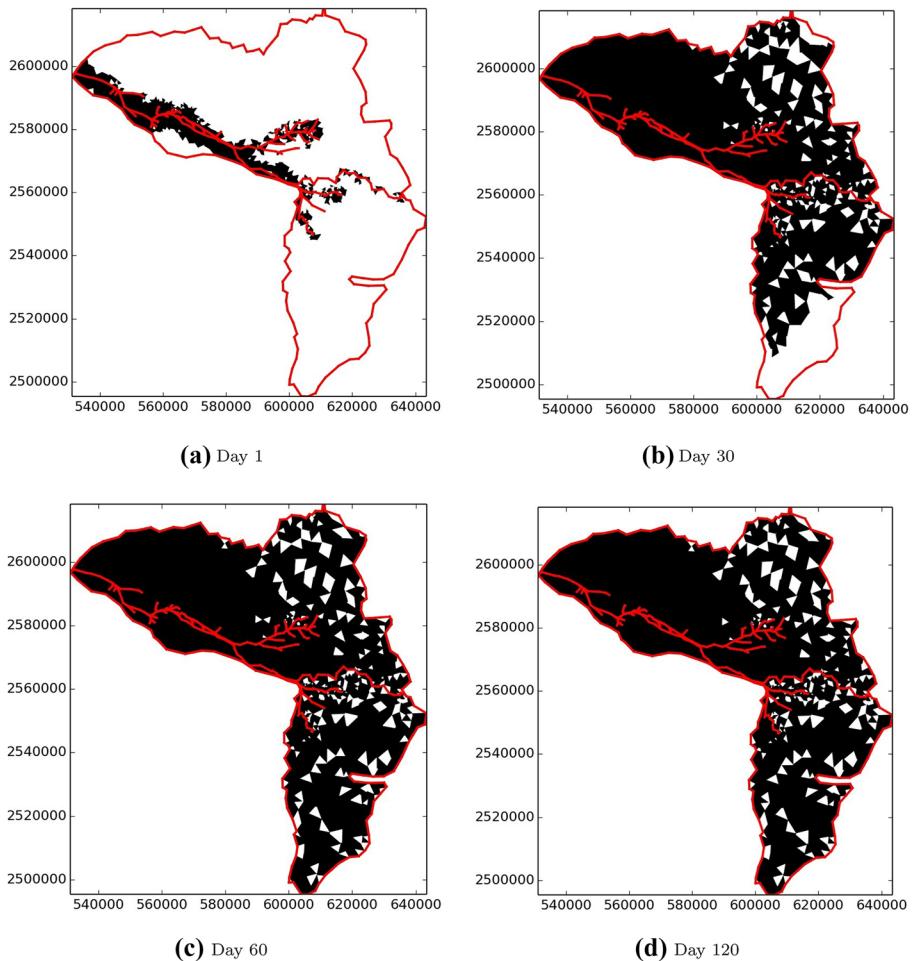

Fig. 4 Progress of water movement for year 2012 using zero-inertia model at the end of **a** Day 1, **b** Day 10, **c** Day 30, **d** Day 40

The cells that do receive water from the canal supply lose some of their water through infiltration which eventually feeds the unconfined aquifer.
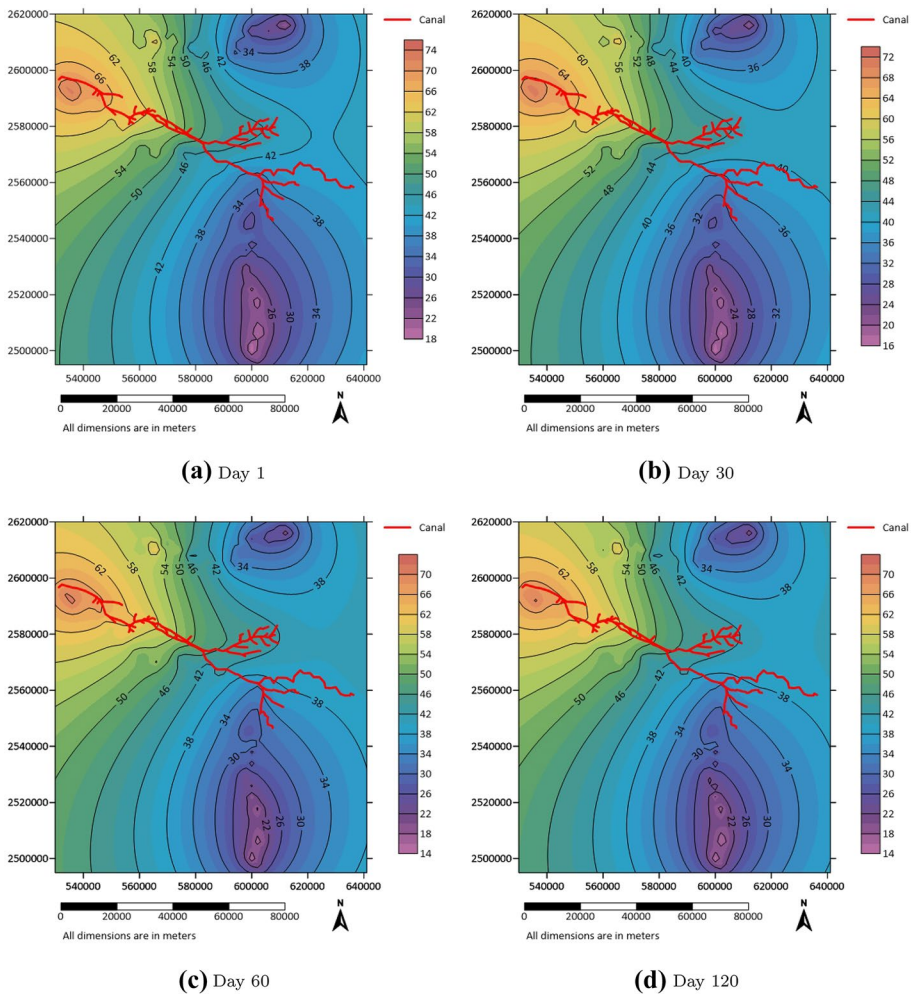
6.1 Canal Regulation Year 2012

The present integrated model for the regulation year 2012 was simulated using 33 canals that include 1 main canal (LBMC) and 32 branch canals. The average of daily discharge values of 120 days (Jan-Apr) was computed which comes out to be around $34 m^3/s$. Total of 3236 UT cells were generated in gmsh (Supplementary Fig. S6-(a)) using its line in surface command. Figure 4 shows the progress of water movement using zero-inertia model (explicit scheme). In the surface inundation graphics, the wet cells with standing water were coloured black and the cells without any standing water were white. Initially, all the spatial

(a) Day 1

(b) Day 30

(c) Day 60

(d) Day 120

Fig. 5 Progress of water movement for year 2012 in the integrated model at the end of **a** Day 1, **b** Day 30, **c** Day 60, **d** Day 120

cells in the model domain were considered to be dry. A minimum positive flow depth value $(10^{-6}m)$ was maintained for dry cells during the simulation. The initial value of water depth (bed elevation $+10^{-6}m$) was specified at each cell to start the numerical simulation.

It can be observed from the results of surface water model for the year 2012 that $\approx 10\%$, 80% and 99% of the area was flooded at the end of 1st, 10th and 30th day whereas, it was completely flooded after 40 days. However, no significant change can be observed even after 30 days. Figure 5 shows the progress of water movement using the integrated model. It may be observed from Fig. 5 that the major change in water wavefront movement is in the initial 30 days when $\approx 70\%$ of the command area was flooded whereas, only 80% of the command area was flooded at the end of 60th day. Furthermore, there are plenty of intermediate dry cells in the integrated model which were not getting flooded even at the end of the simulation period (120th day). This may be due to local slope variation and infiltration

(a) Day 1
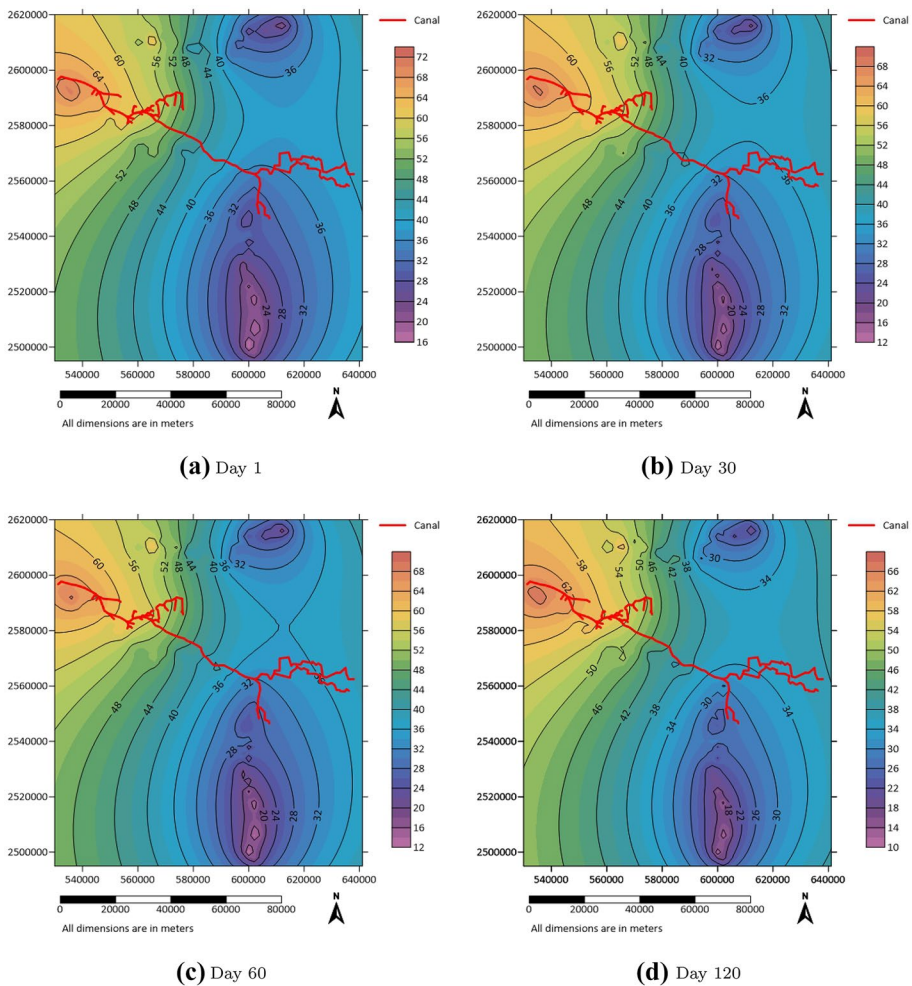
(b) Day 30

(c) Day 60

(d) Day 120

Fig. 6 Contour map of groundwater hydraulic head for year 2012 at the end of **a** Day 1, **b** Day 30, **c** Day 60, **d** Day 120

loss. The groundwater contour maps for the respective time steps (day 1, day 30, day 60 and day 120) are also shown in Fig. 6. In the groundwater contour maps red line indicates the canal regulation map for the year 2012.

6.2 Canal Regulation Year 2013

Present model for the regulation year 2013 was simulated using 21 canals that includes 1 main canal (LBMC) and 20 branch canals. The average of daily discharge values (Jan-Apr) was computed which comes out to be around $22 m^3/s$. Total of 2532 UT cells were generated using gmsh (Supplementary Fig. S6-(b)) for simulation. In 2013 lesser number of canal networks were receiving water supply as compared to 2012. Therefore, the number of cells in 2013 was significantly reduced. It can be observed from the surface water model

(a) Day 1

(b) Day 30

(c) Day 60

(d) Day 120

Fig. 7 Contour map of groundwater hydraulic head for year 2013 at the end of **a** Day 1, **b** Day 30, **c** Day 60, (d) Day 120

for 2013 (Supplementary Fig. S7), that the domain is completely flooded after 50 days and no significant changes were occurring after 30 days.

Integrated model for 2013 (Supplementary Fig. S8) shows a similar pattern of water movement as in 2012. Major changes in water front movement were in the initial 30 days. The groundwater contour maps were also shown in Fig. 7. A considerable decline in hydraulic head values from 2012 to 2013 were also observed which can be justified with the decrease in water supply from 2012 to 2013 and increase in area under Boro rice cultivation. The effect of this change is visible in the groundwater head contour plots. Furthermore, several studies are available which investigate the variation in groundwater levels (Maheswaran et al. 2016; Biswas et al. 2017; Kebede et al. 2021) in command systems. However, AEM was not utilized in them which can deal regional scale problems satisfactorily with limited data sets.

7 Conclusions

As mentioned earlier, the water requirement for Boro rice was not originally considered in the design of the irrigation system and the area under Boro rice cultivation has been typically increasing in the past few decades. As a result, the available canal water is not sufficient to fulfill irrigation requirements in the middle and lower reaches of the command area. Therefore, the farmers are dependent on groundwater to satisfy this demand. From the results obtained for the regulation years 2012 and 2013, the following inferences may be drawn: (a) the efficiency of overland flow movement in the total number of dry/wet cells are influenced by the local slope variation and water lost by infiltration; (2) higher groundwater hydraulic head values were observed in the areas nearer to the canal than those farther away; (3) as the soil considered in the study area is poorly drained, no significant increase in groundwater head values was observed during the first 30 days when maximum number of basin cells were flooded; (4) the influence of a growing crop in depleting the groundwater head (affected by pumping to meet the crop water need) was observed more prominently for the regions away from canals (mid-reach and lower reach) and where the surface cells were dry. A considerable decline in hydraulic head values from 2012 to 2013 were also observed which can be justified with the decrease in water supply from 2012 to 2013 and increase in area under Boro rice cultivation. It magnifies the need for conjunctive water management in canal irrigated areas to increase/improve water use efficiency.

It may also be concluded that a fully-coupled model performs satisfactorily when the groundwater and surface water interactions are needed at the regional scale, with the consideration of all of the hydrological processes. However, the lack of field data in large-scale modelling creates a major hindrance to the successful application of the fully-coupled model. Moreover, the logical conclusions drawn from the analysis carried out, demonstrate that the model responds well to the factors affecting the canal command irrigation scenario and therefore, it can be used in decision-making by the water managers and policymakers of canal irrigated districts. The developed coupled model can be utilized to demarcate areas with maximum groundwater depletion so that a comprehensive water management plan can be suggested to explore the scope of future groundwater development in those areas. It will be helpful to deal with the water shortage faced by local communities in the tail reaches of command area. Moreover, the model may also be refined for further intensive applications by taking into account more realistic processes (e.g., heterogeneous nature of unsaturated medium below the soil surface, temporal as well as spatial variation of recharge/discharge components, varying soil hydraulic parameters).

Declarations

Ethics Approval Not applicable.

Consent to Participate The authors declare their consent to participate in this work.

Consent for Publication The authors have approved the manuscript and its submission to the Journal.

Conflicts of Interest The authors declare that they have no conflict of interest.

References

Ahmad I, Zhang F (2022) Optimal agricultural water allocation for the sustainable development of surface and groundwater resources. Water Resour Manage 36(11):4219–4236

Aricò C, Nasello C (2018) Comparative analyses between the zero-inertia and fully dynamic models of the shallow water equations for unsteady overland flow propagation. Water 10(1):44

Bakker M (2007) Simulating groundwater flow to surface water features with leaky beds using analytic elements. Adv Water Resour 30(3):399–407

Bakker M, Anderson E, Olsthoorn T, Strack O (1999) Regional groundwater modeling of the yucca mountain site using analytic elements. J Hydrol 226(3):167–178

Bandilla K, Janković I, Rabideau A (2007) A new algorithm for analytic element modeling of large-scale groundwater flow. Adv Water Resour 30(3):446–454

Biswas P, Dhar A, Sen D (2017) A numerical simulation model for conjunctive water use in basin irrigated canal command areas. Water Resour Manage 31(12):3993–4005

Brufau P, García-Navarro P, Playán E, Zapata N (2002) Numerical modeling of basin irrigation with an upwind scheme. J Irrig Drain Eng 128(4):212–223

Caviedes-Voullième D, Fernández-Pato J, Hinz C (2020) Performance assessment of 2d zero-inertia and shallow water models for simulating rainfall-runoff processes. J Hydrol 584

Cea L, Garrido M, Puertas J (2010) Experimental validation of two-dimensional depth-averaged models for forecasting rainfall-runoff from precipitation data in urban areas. J Hydrol 382(1–4):88–102

Craig J, Janković I, Barnes R (2006) The nested superblock approach for regional-scale analytic element models. Groundwater 44(1):76–80

De Lange W (1999) A cauchy boundary condition for the lumped interaction between an arbitrary number of surface waters and a regional aquifer. J Hydrol 226(3):250–261

De Lange W (2006) Historical note: Development of an analytic element ground water model of the netherlands. Groundwater 44(1):111–115

Fitts C (1989) Simple analytic functions for modeling three-dimensional flow in layered aquifers. Water Resour Res 25(5):943–948

Geuzaine C, Remacle J (2009) Gmsh: A 3-d finite element mesh generator with built-in pre-and post-processing facilities. Int J Numer Meth Eng 79(11):1309–1331

Hunter N, Horritt M, Bates P, Wilson M, Werner M (2005) An adaptive time step solution for raster-based storage cell modelling of floodplain inundation. Adv Water Resour 28(9):975–991

Jha M, Singh L, Nayak G, Chowdary V (2020) Optimization modeling for conjunctive use planning in upper damodar river basin, india. J Clean Prod 273

Kebede S, Charles K, Godfrey S, MacDonald A, Taylor RG (2021) Regional-scale interactions between groundwater and surface water under changing aridity: evidence from the river awash basin, ethiopia. Hydrol Sci J 66(3):450–463

Kumari K, Dhar A (2020) Groundwater management using coupled analytic element based transient groundwater flow and optimization model. Algorithms and Applications in Science and Engineering, Nature-Inspired Methods for Metaheuristics Optimization, pp 119–134

Maheswaran R, Khosa R, Gosain A, Lahari S, Sinha S, Chahar B, Dhanya C (2016) Regional scale groundwater modelling study for ganga river basin. J Hydrol 541:727–741

Murillo J, García-Navarro P (2010) Weak solutions for partial differential equations with source terms: Application to the shallow water equations. J Comput Phys 229(11):4327–4368

Murray-Rust DH, Vander Velde EJ (1994) Conjunctive use of canal and groundwater in punjab, pakistan: management and policy options. Irrig Drain Syst 8(4):201–231

Omar PJ, Gaur S, Dwivedi S, Dikshit P (2019) Groundwater modelling using an analytic element method and finite difference method: an insight into lower ganga river basin. J Earth Syst Sci 128:1–10

Philipp A, Liedl R, Wöhling T (2012) Analytical model of surface flow on hillslopes based on the zero inertia equations. J Hydraul Eng 138(5):391–399

Playán E, Walker W, Merkley G (1994) Two-dimensional simulation of basin irrigation. ii: Applications. J Irrig Drain Eng 120(5):857–870

Pradhan S, Dhar A, Tiwari KN (2022a) On quantification of groundwater dynamics under long-term land use land cover transition. Water Resour Manage 36(11):4039–4055

Pradhan S, Dhar A, Tiwari KN, Sahoo S (2022b) Spatiotemporal analysis of land use land cover and future simulation for agricultural sustainability in a sub-tropical region of India. Environ Dev Sustain pp. 1–30

Rawls WJ, Brakensiek DL, Miller N (1983) Green-ampt infiltration parameters from soils data. J Hydraul Eng 109(1):62–70

Schmitz G, Seus G (1992) Mathematical zero-inertia modeling of surface irrigation: Advance in furrows. J Irrig Drain Eng 118(1):1–18

Strack O (1989) Groundwater mechanics. Prentice Hall, Eaglewood Cliff, New Jersey

Strack O (2003) Theory and applications of the analytic element method. Rev Geophys 41(2)

Strack O (2006) The development of new analytic elements for transient flow and multiaquifer flow. Groundwater 44(1):91–98

Tong C, Wang C, Xiong M, Huang CS, Yeh HD (2023) An analytical and meshless model for 3d transient flow in a confined aquifer with nonuniform thickness: Application to stream depletion due to groundwater extraction. Environ Model Software 159

Valipour M (2012) Comparison of surface irrigation simulation models: full hydrodynamic, zero inertia, kinematic wave. J Agric Sci 4(12):68

Zapata N, Playan E (2000) Simulating elevation and infiltration in level-basin irrigation. J Irrig Drain Eng 126(2):78–84

Zhang S, Xu D, Bai M, Li Y, Xia Q (2014) Two-dimensional zero-inertia model of surface water flow for basin irrigation based on the standard scalar parabolic type. Irrig Sci 32(4):267–281

Zhang S, Bai M, Xia Q, Yu H (2017) Efficient simulation of surface water flow in 2d basin irrigation using zero-inertia equations. J Irrig Drain Eng 143(1):04016069

Zhao J, Liang Q (2022) Novel variable reconstruction and friction term discretisation schemes for hydrodynamic modelling of overland flow and surface water flooding. Adv Water Resour 163